Communication in Physical Sciences, 2025, 12(2) 353-366

Isolation and Synthesis of Cellulose Nanofibers From Cassava Inner Peel Using Phosphoric Acid

Usman Ibrahim, Musa Muhammad, Azeh Yakubu and Umar Muhammad Badegi..
Received: 12 December 2024/Accepted 24 January 2025/Published 05 February 2025
https://dx.doi.org/10.4314/cps.v12i2.13

Abstract: *This study presents the synthesis and characterization of nanomaterial as a prerequisite for its efficient use in water purification as an alternative to costly activated carbon. Here, solvent-free phosphorylation of nanocellulose using environmentally benign and non-toxic chemicals was pursued resulting in a negatively charged material that was used to remove pollutants. The native material was locally abundant cassava inner peel biowastes which is rich in cellulose fibers. Native cellulose was isolated from the inner peel cassava waste and subsequently, hydrolyzed using phosphoric acid at 200 ^{o}C for 1 h on a sand bath at a cellulose/acid ratio of 1 g:25 mL. to afford nanocellulose fibre. The native cellulose was isolated, and the phosphorylated nanocellulose fibre was characterized using scanning electron microscope (SEM), Fourier transforms infrared (FT-IR), thermo-gravimetric analyzer (TGA/DTG) and Brunauer-Emmett-Teller (BET), for its surface features, and functionalities, thermal stability, surface area, and particle size, respectively. SEM analysis revealed highly irregular and tiny individualized nanofiber strands, indicating the presence of nanocellulose fibre. The surface area of the cellulose and nanocellulose was 219.637 m^2/g and 299.478 m^2/g with pore volumes of 0.108 and 0.146 cm^3/g.*

Keywords: *Cassava peel Cellulose, Nanocelluloses, SEM, TGA, BET*

Usman Ibrahim*
Ibrahim Badamasi Babangida University,
Department of Chemistry, Lapai, Niger State, Nigeria
Email: ibrahimibrahimg16@gmail.com
Orcid id: 0009-0004-3025-4981

Musa Muhammad
Ibrahim Badamasi Babangida University,
Department of Chemistry, Lapai, Niger State, Nigeria
Email: contactdrmusa@gmail.com
Orcid id: 0000000233027686

Yakubu Azeh
Ibrahim Badamasi Babangida University,
Department of Chemistry, Lapai, Niger State, Nigeria
Email: azehy@ibbu.edu.ng
Orcid id: 0000-0002-3818-674X

Muhammad Umar Badeggi
Ibrahim Badamasi Babangida University,
Department of Chemistry, Lapai, Niger State, Nigeria
Email: umb2016@gmail.com
Orcid id: 0000-0003-4774-4237

1.0 Introduction

Industrialization and human activities have led to an increasing number of pollutants entering water resources (Eddy *et* al., 2024a-b). Amongst these, pollutants are full of aromatic, toxic, and hardly biodegradable chemicals thus challenging industrial wastewater treatment and hazarding the environment (Lellis *et al.* 2019). To satisfy demands in the environment alone, 10 000 different pollutants amounting to some 7 9 10 5 tons are released each year, while partially ending up in waste stream discharges (He *et al.* 2013). In addition, other dye-consuming industries such as pulp and paper, pharmaceutical, and tannery are also responsible for dye discharges into the environment (Eddy *et* al., 2023a-b; He *et al.* 2013). This has prompted many research

activities aiming to develop inexpensive, efficient, and sustainable purification technologies that could tackle dye-contaminated water (Rafatullah *et al.* 2010). Adsorption seems to offer the best prospects over other water treatment methods such as coagulation and precipitation which make use of intensive chemical treatments and result in residuals that require further treatment (Bolisetty and Mezzenga 2016). Although adsorption technologies such as activated carbon are effective and highly used for water remediation, they remain costly and difficult to regenerate, and this hampers their economical usage. Ideal alternatives would be sustainable, low-cost, high-capacity adsorbents derived from locally abundant natural substances (Han *et al.* 2010; Sharma *et al.* 2011; Gupta *et al.* 2013; Udongwo & Folorunso, 2025). Cellulose, the most abundant natural polymer on earth, is undoubtedly one of the most attractive materials for designing water purification adsorbents due to its worldwide availability, renewability, benign character, facile surface modification, and processing versatility (Carpenter *et al.* 2015; Sehaqui *et al*. 2016b). To tackle the low/moderate adsorption properties of native cellulose, active functional groups are attached to its backbone allowing the immobilization of charged pollutants and non-polar species (Sehaqui 2014, 2016a, b). For instance, carboxylate or phosphate-modified cellulose filters and membranes have been effectively used for the uptake of positively charged dyes and heavy metal ions (Ma *et al.* 2012; Blilid *et al*. 2019; Lehtonen *et al.* 2020). Over the past years, increased interest in cellulose phosphorylation as a promising route for the introduction of negative charges has been reborn, mainly concerning its utilization for nanocellulose production, flame retardancy, and water purification (Ghanadpour *et al*. 2015; Lehtonen *et al.* 2020). Although cellulose phosphorylation can proceed in various media (e.g., DMF (Granja *et al*. 2001), DMAc/LiCl (Aoki and Nishio 2010), pyridine (Reid *et al.* 1949)) using various phosphorus based-chemicals [e.g., H_3PO_4 (Reid *et al.* 1949; Suflet *et al*. 2006), P_2O_5 (Granja *et al*. 2001), $POCl_3$ (Reid *et al.* 1949)], and at various operating conditions, the reaction with mono-ammonium and di-ammonium phosphate in the presence of urea at 150–165°C seems to offer the best prospects as a green, simple and inexpensive route resulting in high functionalization degree and relatively low cellulose degradation. Application possibilities of phosphorylated (nano)cellulose include flame-retardancy, water purification, and many others (Noguchi *et al.* 2017; Ghanadpour 2018).In the area of water purification, phosphorylated cellulose is used for its adsorption properties towards positively charged pollutants, mainly heavy metal ions and dyes. Here, the aim is to achieve similar adsorption properties to well-known commercial sorbents such as activated carbon. In a study by Sunflet *et al.* (2017), phosphorylated cellulose microspheres were used for the uptake of methylene blue (MB) from an aqueous solution. The microspheres displayed both a low exchange capacity of 0.24 meq/g^{-1} and a low adsorption capacity towards MB (about 60 mg/g^{-1}) (Suflet *et al.* 2017). In another study by Luo *et al.*, phosphorylated cellulose microspheres were applied for the effective chelation of Pb_2 in aqueous media, and an adsorption capacity of 108 mg/g^{-1} was reached (Luo *et al.* 2017). Srivastava *et al*. reported an adsorption capacity ranging from 25–70 mg/g^{-1} of various metal ions (Cu_2, Ni_2, Cd_2, and Pb_2) onto phosphorylated cellulose triacetate-silica composites (Srivastava *et al*. 2016). Oshima *et al*. and Zhuang *et al*. utilized phosphorylated bacterial cellulose as an adsorbent for metal ions and registered a good adsorption behaviour for various transition metal ions, lanthanide ions, and U (VI) via ion-exchange mechanism (Oshima *et al.* 2008; Zhuang and Wang 2019). The phosphorylated

nanocellulose paper was used to filter heavy metal ions such as Cu_2 from an aqueous solution, although the nano paper's charge content (18.6 mmol/kg^{-1}) and the flux registered remained low (Mautner *et al.* 2016). Recently, Lehtonen *et al.* showed a great adsorption capacity of radio-active uranium species onto phosphorylated cellulose (1550 mg/g^{-1}), provided by the high concentration of phosphoryl groups attached to the cellulose (1 mmol g^{-1}) (Lehtonen *et al*. 2020). Despite these numerous studies, the potential of phosphorylated cellulose as a promising dye adsorbent has not yet been demonstrated. In this work, we aim to investigate the chemical characteristics and sorption properties of phosphorylated nanocellulose made of locally abundant resources using a straightforward phosphorylation process with Phosphoric acid. A fast-growing plant thriving in dry regions of North Africa and covering a large area of about 3 million hectares in Morocco (named Alfa grass, Esparto or *Stipa tenacissima*) (El Achaby *et al.* 2018) has been selected as a cellulose source together with commercial wood fibres and microcrystalline cellulose, were investigated and compared to the state of the art sorbents reported in the literature to conclude the potential of the present bio-based material for water purification. To the best of our knowledge, amongst all phosphorylated biopolymers reported to date, the present phosphorylated cellulose materials achieved unprecedented adsorption capacity against methylene blue comparable to the capacity achieved by the best-activated carbon sorbents.

2.0 Materials and Method

2.1 Material

Cassava peel (CP) was collected from a cassava farm Lapai Niger state, Nigeria. The chemicals used for cellulose isolation and nanocellulose preparation were: distilled water, sodium hypochlorite, sodium hydroxide, ethanol, n-hexane, acetate, concentrated H_3PO_4, pure microcrystalline cellulose (analytical grade).

2.2 Sample Preparation

2.2.1 Isolation of Cellulose;

Chemically purified cellulose (CPC) from cassava peel was isolated according to the previously reported methods (Filpponen 2009, Rosa *et al*. 2010; Jabbar and Timell 1960). Prior to cellulose isolation, cassava peel was separated from its outer skin, washed and milled into pulp. This pulp was then dried in sunlight for 2 days until a constant weight was obtained. (Sulphuric/phosphoric methods) 10 g of dried pulp was dissolved in a mixture of ethanol/n-hexane/acetate (1:1:1) which was allowed to stand for 48 hrs. The mixture was decanted and 200 mL of 0.5M H_2SO_4/H_3PO_4 was added and heated at 90° C for 2 h with constant stirring. Subsequently, the mixture is filtered and the obtained residue is washed until neutral. The next step is a bleaching process wherein the residue is refluxed using 2 % $NaClO_2$ solution plus a few drops of glacial acetic acid for 30 minutes.

2.2.2 Preparation of Nanocellulose

Produced CPC was then used to extract CNCs by acid-hydrolysis. Isolated cellulose from cassava peel was hydrolyzed with sulfuric acid in a ratio of cellulose to sulfuric acid (1:25). The hydrolysis of cellulose was carried out in 45 % (w/w) phosphoric acid solution at 200 ^{o}C for 1 hr. The hydrolysis process was quenched by adding excess distilled water (250 mL) to the reaction mixture. The produced colloidal suspension was centrifuged at 14,000 rpm for 10 minutes at -4^{o} C. Then, it was dialyzed for 5 days to neutralize and eliminate the sulfate ions. The neutral colloidal suspension was sonicated for 30 minutes to homogenize the generated nanocellulose.

2.3 Characterization of Adsorbent

2.3.1 Scanning Electron Microscopy (SEM)

The morphology of the cellulose and nanocellulose surface was determined using the Scanning Electron Microscope (SEM) that was equipped with Energy Dispersive X-ray

spectra (EDX) to also determine the elemental composition. About 0.02 mg was suspended in 1 ml of CH_3OH. The mixture was then sonicated for 10.0 minutes followed by a coating of 2 drops of the sample with gold using a gold sputtering device. The SEM images were then obtained on a FEG 450 SEM operating at 80kV.

Plate 1a; dried cassava peel

Plate 1b; grounded cassava peel

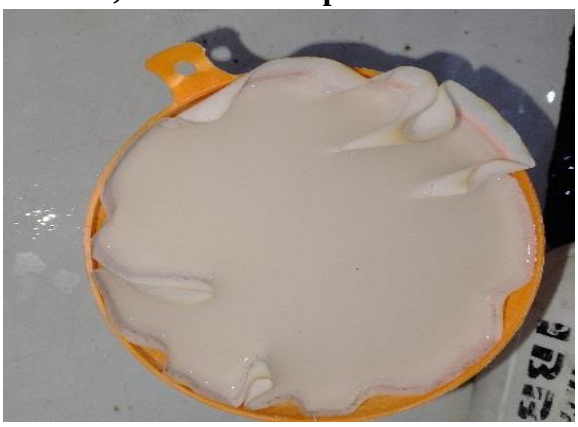

Plate 1c; filter cellulose

Plate 1d; Nanocellulose

2.3.2 Fourier Transform Infrared (FTIR)

The cellulose and nanocellulose sample was mixed with KBr before being compressed into a pellet of 1.0 mm thick. Perkin-Elmer spectrometer (Spectrum one) was employed for the analysis of the sample. The FTIR spectra of the prepared cellulose and nanocellulose were recorded from 450-4000 cm^{-1} (Ettish *et al.*, 2021).

2.3.3 Thermogravimetric Analysis (TGA)

The thermal property of the cellulose and nanocellulose was studied as a function of temperature using thermogravimetric Analysis (TGA). It was done under a nitrogen atmosphere and a purge gas flow rate of 50 cm^3/min and a temperature of 25 to 800 °C. 10 mg of prepared cellulose and nanocellulose was heated at the heating rate of 10 °C min^{-1}.

2.3.4 BET Surface Area

The Brunauer-Emmett-Teller analysis was employed to determine the porosity and surface area of the sample. 300 mg of the sample was degassed for 4 hours at 150°C under nitrogen gas flow to eliminate moisture and other impurities. Nitrogen gas was used as adsorbate and analysis was done at -196°C with NOVA 4200e Quantachrome analyzer.

2.3.5 Rama spectral

Horiba Jobin Yvon LabRAM HR; this spectrometer is considered one of the most advanced and versatile Raman instruments available. It offers: High spectral resolution (down to 0.5 cm^{-1}), High sensitivity, Wide spectral range (100-4000 cm^{-1}), Advanced confocal microscopy capabilities, Ability to handle various sample types (liquids, solids, powders, etc.) and User-friendly software and data analysis tools.

3.0 Results and Discussion

3.1 SEM Study of Samples

The SEM analysis of isolated cellulose and cellulose nanofibers revealed significant differences in their morphology and dimensional characteristics. The SEM images shown in Plates 2a and 2b highlight the fibrous-like network structure of both cellulose and cellulose nanofibers. However, a notable reduction in fiber length is observed in the cellulose nanofibers compared to the native cellulose. The nanofibers' length decreased substantially, from 100–300 nm to 20–100 nm, due to the increased acid concentration used during synthesis.

In the native cellulose, minimal differences in morphology and dimension were observed between samples, with fibers consistently measuring 100–300 nm in length and 10–30 nm in width. This contrasts with the cellulose nanofibers, which exhibit smaller nanoscale dimensions. The reduction in fiber size and morphological changes in the nanofibers can be attributed to NaOH treatment, as suggested by Jin et al. (2016) and Neto et al. (2016). This treatment induces the rearrangement of cellulose chains through hydroxide ions' orientation and removal of non-cellulosic components from the cellulose matrix.

The SEM images of cellulose nanofibers reveal a web-like morphology with hollow features, indicating the removal of hemicelluloses and non-structural cellulose during the process. This transformation, facilitated by ultrasonic-assisted hydrolysis with mixed acid (Wang et al., 2007), results in cellulose chains folding and packing in an anti-parallel configuration, forming a more stable structure. The porous network observed on the surface of the cellulose nanofibers enhances their high porosity and surface area-to-volume ratio. These features make nanofibers potentially useful for pollutant removal, as the heterogeneous pore distribution could enable selective adsorption of molecules based on size and chemical properties (Lay et al., 2020). This distinctive morphology, characterized by rough texture and interconnected pores, underscores the advantages of cellulose nanofibers over native cellulose in applications requiring high surface reactivity and adsorption capacity.

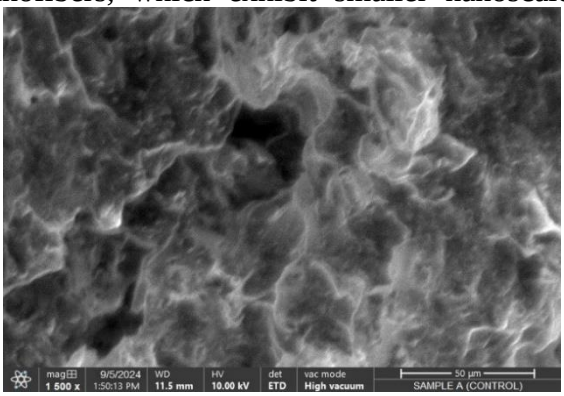

A

Plate 2a: SEM Image of Cellulose

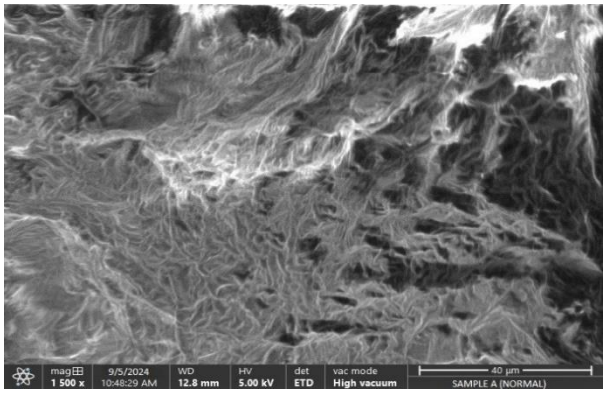

b

Plate 2b: SEM Image of Nanocellulose Fiber

3.2 FT-IR Study of Samples

The FT-IR spectra of cellulose (Fig. 1) and cellulose nanofiber (Fig. 2) show distinct differences in peak positions and intensities, reflecting changes in molecular structure and functional groups. Peaks observed between 991–760 cm^{-1} in the FT-IR spectrum of cellulose are attributed to C-H and C-O stretching vibrations, which are characteristic of the cellulose backbone (Liu, 2018). This band is also present in the spectrum of cellulose nanofiber but exhibits shifts, indicating structural modifications during the synthesis process. The band between 1364–1077 cm^{-1}, assigned to C-O-C glycosidic bond vibrations, is an indication of crystalline cellulose. This peak is prominent in both cellulose and cellulose nanofiber spectra, confirming the preservation of the glycosidic linkage (Wang, 2019).

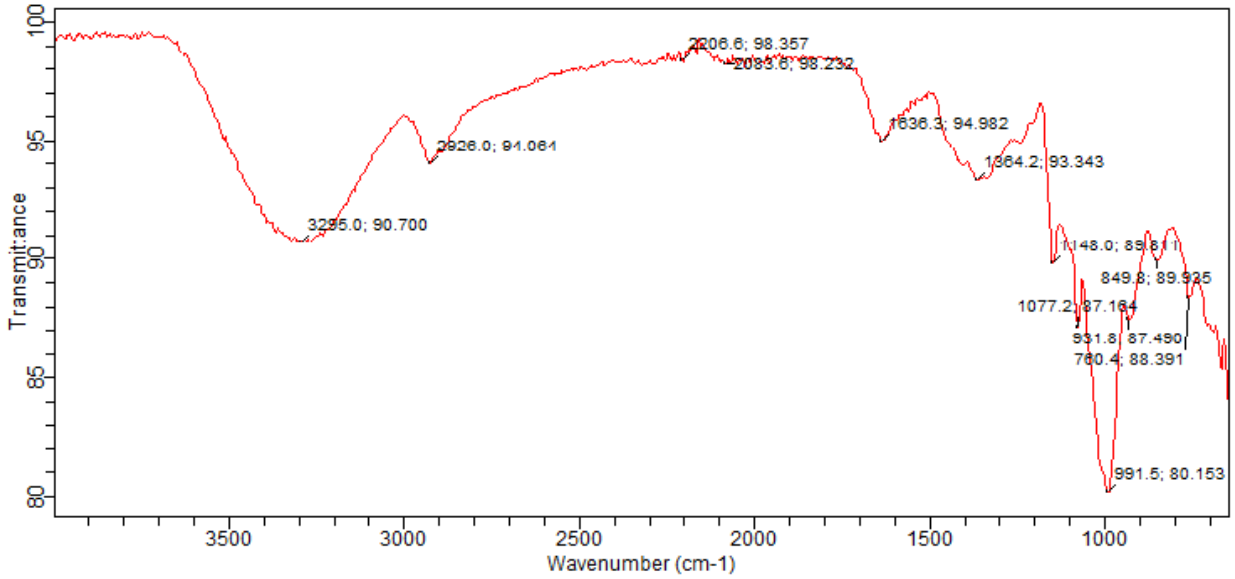

Fig. 1: FTIR Spectra of Cellulose

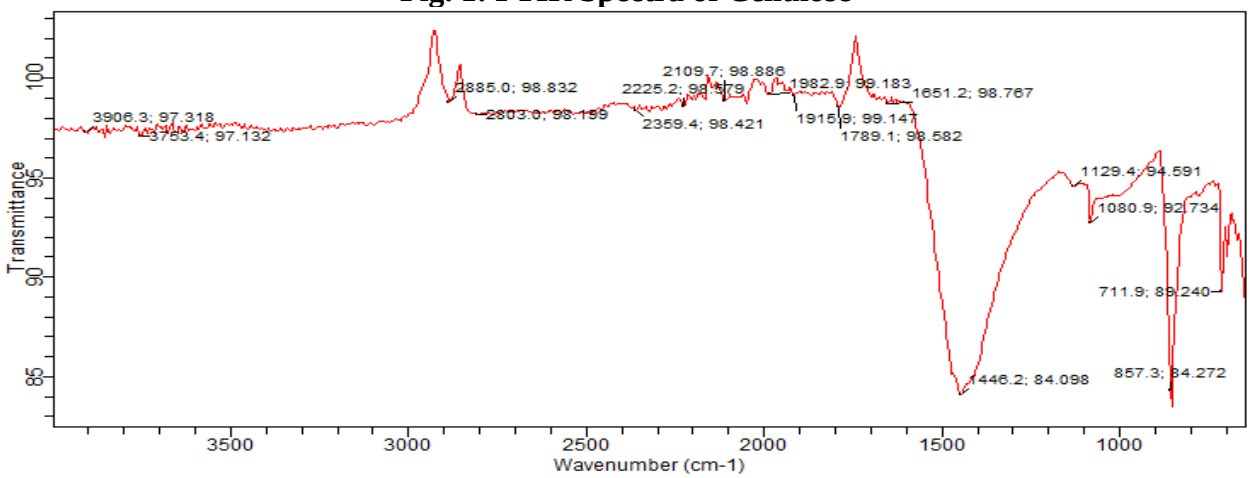

Fig. 2: FTIR Spectra of Nanocellulose

Peaks around 2083–1636 cm^{-1} are associated with O-H bending and C=O stretching vibrations, which suggest the presence of hydroxyl groups and carbonyl moieties (Sreekumar, 2018). These bands appear in both spectra but show variations in intensity,

reflecting molecular rearrangements during nanofiber formation. Absorptions in the range of 2926–2206 cm^{-1} are attributed to C-H stretching vibrations, indicating the presence of alkyl chains. These peaks are detected in both spectra, with variations in intensity signifying the structural refinement of cellulose nanofiber (Liu, 2018). In cellulose nanofiber, peaks observed between 1129–711 cm^{-1} are assigned to C-H, C-O-C, C-OH, and C-C vibrations due to glycosidic linkages in the cellulose backbone. Shifts in these peaks compared to native cellulose indicate alterations in the molecular structure during nanofiber synthesis (Panda, 2017). Peaks recorded at 1789–1446 cm^{-1} in the nanofiber spectrum correspond to C=O and C-O stretch vibrations, suggesting the presence of natural acetate groups ($COOCH_3$) (Wang, 2019). These new peaks are not observed in the cellulose spectrum, highlighting chemical modifications during the nanofiber isolation process.

Absorptions between 2359–1915 cm^{-1} in the nanofiber spectrum are attributed to changes in molecular conformation and hydrogen bonding. This indicates the development of a more organized hydrogen-bonded structure in cellulose nanofiber compared to native cellulose (Sreekumar, 2018). The broad band observed around 3906–2803 cm^{-1} is assigned to surface functional groups, such as bonded (-OH) and asymmetric C-H stretching vibrations from CH_2 groups in the cellulose backbone. This band confirms the introduction of additional functional groups during the conversion to nanofibers (Panda, 2017).

Table 1: FT-IR Band Assignment of Native Cellulose Based on Related Literature

Wavenumber (cm^{-1})	Band Assignment (Functional Group)	Reference	Reference Standard (cm^{-1})
2926–2206	C-H stretching vibrations, indicating alkyl chains	Liu, 2018	2850–2960
2083–1636	O-H bending and C=O stretching vibrations, suggesting hydroxyl groups and carbonyl moieties	Sreekumar, 2018	1630–1680
1364–1077	C-O-C glycosidic bond vibrations, indicating crystalline cellulose	Wang, 2019	1200–1360
991–760	C-H and C-O stretching vibrations, characteristic of cellulose	Liu, 2018	800–1100

Table 2: FT-IR Band Assignment of Cellulose Nanofiber Based on Related Literature

Wavenumber (cm^{-1})	Band Assignment (Functional Group)	Reference	Reference Standard
3906–2803	Bonded (-OH) and C-H stretching vibration due to CH_2 (methylene of the cellulose backbone)	Panda, 2017	2800–3800
2359–1915	Increased intensity and new peaks indicating changes in molecular conformation and hydrogen bonding	Sreekumar, 2018	1900–2400

1789–1446	C=O and C-O stretch vibration due to natural acetate ($COOCH_3$)	Wang, 2019	1700–1800
1129–711	C-H, C-O-C, C-OH, C-C vibrations due to glycosidic linkage and the cellulose backbone; shifted positions indicate altered molecular structure	Panda, 2017	700–1200

3.3 TGA Analysis

The TG and DTG curves of cellulose and nanocellulose, presented in Fig.s 3a and 3b, illustrate distinct weight loss patterns. In the low-temperature range (<105 °C), an initial small weight loss for all samples corresponds to the evaporation of absorbed water. This weight loss is slightly more pronounced for cellulose nanofiber (CNF) due to its higher surface area and the presence of more hydroxyl groups, which allow for increased moisture adsorption.

As shown in Fig.s 3a and 3b, the weight loss trends of native cellulose and cellulose nanofiber are generally similar. Both materials exhibit pronounced thermal degradation starting at approximately 200–250 °C.

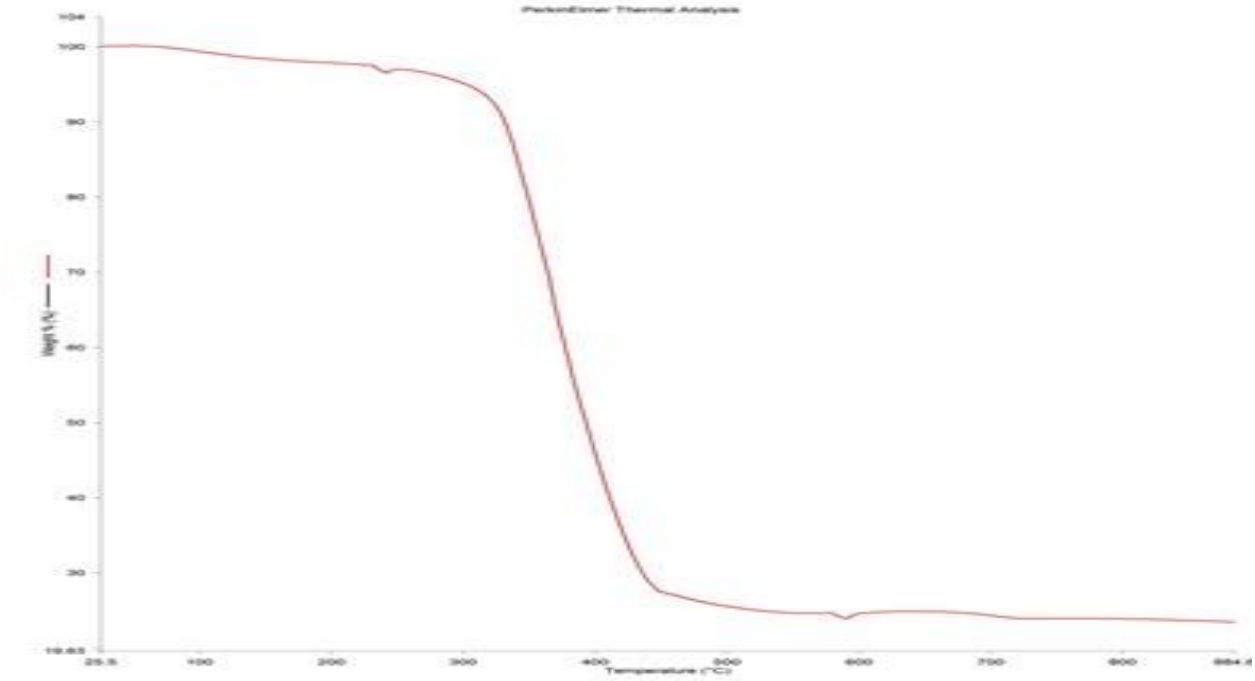

Fig. 3a: TGA of cellulose

However, the main decomposition for cellulose begins near 350 °C, with maximum degradation observed at 410 °C. In contrast, the cellulose nanofiber undergoes maximum degradation at a slightly higher temperature of 420 °C. This shift indicates that nanocellulose, despite its reduced crystallinity, retains some thermal stability due to its altered molecular structure and smaller particle size.

The degradation process for both cellulose and nanocellulose is completed by approximately 450 °C, leaving behind minimal char residue. Despite changes in polymorphs, both cellulose and nanocellulose exhibit comparable thermal degradation behavior in terms of their overall

pattern. However, the thermal degradation behavior of cellulose nanofibers is more complex, as shown in Fig. 3b. This complexity is attributed to the smaller particle size, greater surface reactivity, and potential surface modifications of the nanocellulose, which lead to additional degradation pathways. These findings suggest that while cellulose and nanocellulose share a similar degradation profile, the unique properties of nanocellulose, such as higher surface area and altered molecular conformation, contribute to nuanced differences in their thermal behavior.

.

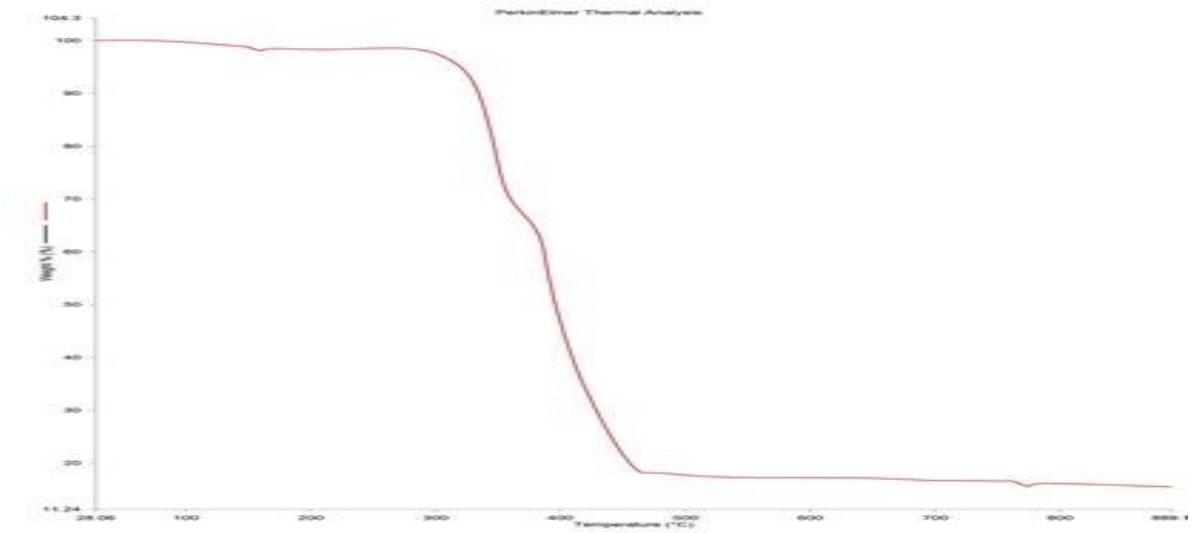

Fig. 3b: TGA of nanocellulose

3.4 BET Analysis

The BET analysis results of the cellulose and cellulose nanofiber showing a specific surface area (SSA) of 219.637 m²/g and 299.478 m²/g are shown in Table 3. This indicates abundant adsorption sites crucial for gas purification, water treatment, and catalysis applications. The reported pore volume of 0.108 cm^3/g and 0.146 cm^3/g suggests a high adsorption capacity, beneficial for removing molecules or ions. The specified pore size of 2.113 nm and 2.153 nm indicates mesoporous characteristics, ideal for effective adsorption of medium-sized molecules. This versatility allows the cellulose and cellulose nanofiber to target a wide range of contaminants, reflecting its suitability for diverse environmental and industrial uses (Gayathiri *et al.,* 2022). these materials are partially hydrophilic.

Table 3: Surface properties based on BET surface area

Material	Surface area (m^2/g)	Pore volume (cm^3/g)	Pore size (nm)
Cellulose	**219.64**	**0.108**	**2.11**
Nanocelulose	**299.48**	**0.146**	**2.15**

The porosity of the cellulose nanofiber makes it plausible to utilize it for inundating huge natural and inorganic materials like molecules, ions and atoms that may be present in water/wastewater not only on their surfaces but throughout the bulk of the material by selective adsorption. Since

3.6 Raman Spectral Analysis

The Raman spectrum of cellulose nanofiber isolated from cassava peel exhibits distinct vibrational modes characteristic of cellulose. A prominent peak at 312 cm^{-1}, with a strong intensity of 1100, is attributed to the C-O-C glycosidic bond vibration in cellulose

(Sreekumar, 2018). This observation aligns with previous studies on cellulose-based materials. For instance, Liu (2018) reported a similar peak for cellulose nanocrystals at 312 cm^{-1} with an intensity of 1100, while Wang (2019) observed a peak at 315 cm^{-1} with an intensity of 900 for cellulose nanofibers. Additionally, Panda (2017) noted a band at 308 cm^{-1} with an intensity of 1200 for bacterial cellulose.

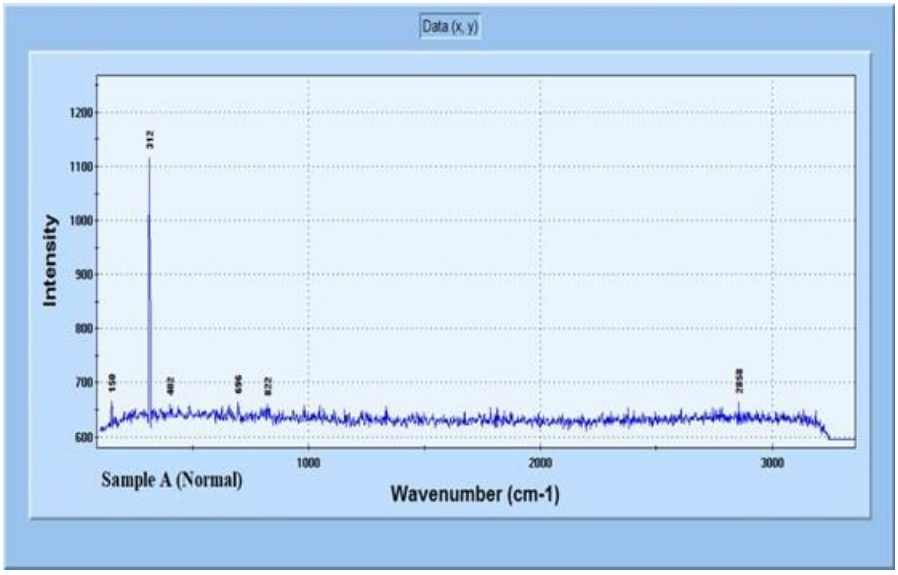

Fig. 5: Raman Spectral of Cellulose Nanofiber from Cassava Peel

The similarity in peak position and intensity across these studies suggests that the cellulose nanofiber material is composed of well-organized cellulose chains with a high degree of crystallinity (Fig. 5). The sharpness of the peak at 312 cm^{-1} indicates a structurally ordered material, consistent with the crystalline nature of cellulose nanofibers. Other peaks in the spectrum include those at 462 cm^{-1} and 690 cm^{-1}, which correspond to bending and symmetric stretching vibrations of glycosidic bonds and C-O-C linkages in cellulose. The peak at 2858 cm^{-1} is associated with C-H stretching vibrations in the aliphatic chains of cellulose. These additional peaks further confirm the structural features of cellulose.

The strong and distinct spectral features of the cellulose nanofibers indicate successful isolation from cassava peel, with minimal interference from non-cellulosic components such as lignin or hemicellulose. The high degree of crystallinity observed is advantageous for potential applications, such as reinforcement in biopolymer composites, filtration, or as a functional material in advanced applications. In summary, the Raman spectrum of cellulose nanofibers from cassava peel confirms the material's high purity and crystalline structure, in agreement with the findings of earlier researchers on similar cellulose-based materials.

4.0 Conclusion

The study demonstrated the synthesized cellulose nanofiber from native cellulose isolated from cassava inner peel and characterized. Results show that both the native cellulose and cellulose nanofiber had particles within the nanoscale dimension. Both celluloses featured properties beneficial for pollutant removal and thermal stability enhancement. The method is simple and easy to implement for the synthesis of

phosphorylated cellulose nanofiber with a large surface area.

5.0 Acknowledgment

I sincerely appreciate the contributions of my supervisors Musa Muhammad, Yakubu Azeh, and Umar Muhammad Badeggi for their support and encouragement. The Technologists of the Department of Chemistry, IBB University, Lapai are appreciated for their unwavering technical support.

6.0 References

Aoki, D., & Nishio, Y., (2010). Phosphorylated cellulose propionate derivatives as thermoplastic flame resistant/retardant materials: Influence of region selective phosphorylation on their thermal degradation behavior. *Cellulose* 17, pp. 963–976. https://doi.org/10.1007/s10570-010-9440-8.

Blilid, S., Katir, N., & El Haskouri, J., (2019). Phosphorylated micro- vs. nano-cellulose: a comparative study on their surface functionalization, growth of titanium-oxo-phosphate clusters and removal of chemical pollutants. *New J Chem* 43, pp. 15555–15562. https://doi.org/10.1039/c9nj03187a.

Bolisetty, S., & Mezzenga, R., (2016). Amyloid-carbon hybrid membranes for universal water purification. Nat Nanotechnol 11, pp. 365–371. https://doi.org/10.1038/nnano.2015.310.

Carpenter, A. W., De Lannoy, C. F., & Wiesner, M. R., (2015). Cellulose nanomaterials in water treatment technologies. *Environ Sci Technol* 49, pp. 5277–5287. https://doi.org/10.1021/es506-351r.

De Menezes, A. J., (2019). Nanocellulose from cassava peel: Extraction, characterization, and application. *Carbohydrate Polymers*, 223, pp. 115-123.

Eddy, N. O., Oladede, J., Eze, I. S., Garg, R., Garg, R., & Paktin, H. (2024a). Synthesis and characterization of CaO nanoparticles from periwinkle shell for the treatment of tetracycline-contaminated water by adsorption and photocatalyzed degradation. *Results in Engineering*, *103374*. https://doi.org/10.1016/j.rineng.2024.103374.

Eddy, N. O., Jibrin, J. I., Ukpe, R. A., Odiongenyi, A., Iqbal, A., Kasiemobi, A. M., Oladele, J. O., & Runde, M. (2024b). Experimental and Theoretical Investigations of Photolytic and Photocatalysed Degradations of Crystal Violet Dye (CVD) in Water by oyster shells derived CaO nanoparticles (CaO-NP), *Journal of Hazardous Materials Advances*, 13, 100413, https://doi.org/10.1016/j.haz - adv.2024.100413.

Eddy, N. O., Edet, U. E., Oladele J. O., Kelle, H. I., Ogoko. E. C., Odiongenyi, A. O., Ameh, P., Ukpe, R. A., Ogbodo, R., Garg, R. and Garg, R. (2023a). Synthesis and application of novel microporous framework of nanocomposite from trona for photocatalysed degradation of methyl orange dye. *Environmental Monitoring and Assessment*. doi : 10.1007/s10661-023-12014-x,

Eddy, N. O., Ukpe, R. A., Garg, R., Garg, R., Odionenyi A. O., Ameh, P. and Akpet, I, N. (2023b). Enhancing Water Purification Efficiency through Adsorption and Photocatalysis: Models, Application and Challenges. *International Journal of Environmental Analytical Chemistry*, doi: 10.1080/03067319.2023.2295934

El Achaby, M., Kassab, Z., Barakat, A., & Aboulkas, A., (2018). Alfa fibers as viable sustainable source for cellulose nanocrystals extraction: Application for improving the tensile properties of biopolymer nanocomposite films. *Ind*

Crops Prod 112, pp. 499–510. https://doi.org/10.1016/j.indcrop.2017.12.049.

Ettish, M. N., El-Sayyad, G. S., Elsayed, M. A., & Abuzalat, O. (2021). Preparation and characterization of new adsorbent from Cinnamon waste by physical activation for removal of Chlorpyrifos. *Environmental Challenges*, 5, 100208. https://doi.org/10.1016/j.envc.2021.100208.

Fa´varo-Polonio, B., Pamphile, C. Z., & Polonio, J. C., (2019). Effects of textile dyes on health and the environment and bioremediation potential of living organisms. *Biotechnol Res Innov* 3:275–290. https://doi.org/10.1016/j.biori.2019.09.001.

Filpponen, I., (2009). *The synthetic strategies for unique properties in cellulose nanocrystals materials:* A dissertation submitted to the Graduate Faculty of North Carolina State University In partial fulfillment of the Requirements for the degree of Doctor of Philosophy Wood & Paper Science Raleigh, North Carolina.

Ghanadpour, M., (2018). *Phosphorylated cellulose nanofibrils: a nano-tool for preparing cellulose-based flame-retardant materials*. PhD Thesis. KTH—Stockholm.

Ghanadpour, M., Carosio, F., Larsson, P. T., & Wa˚gberg, L., (2015). *Phosphorylated Cellulose Nanofibrils: A Renewable Nanomaterial for the Preparation of Intrinsically Flame- Retardant Materials*. *Biomacromol* 16, pp. 3399–3410. https://doi.org/10.1021/acs.biomac.5b01117.

Granja, P., Poulyse´gu, L., & Pe´traud, M. (2001). Cellulose phosphates as biomaterials. I. Synthesis and characterization of highly phosphorylated cellulose gels. *J Appl Polym Sci*, 82, pp. 3341–3353. https://doi.org/10.1002/app.2193.

Gayathiri, M., Pulingam, T., Lee, K. T., & Sudesh, K. (2022). Activated carbon from biomass waste precursors: Factors affecting production and adsorption mechanism. *Chemosphere*, 294, pp. 133764. https://doi.org/10.1016/j.chemosphere.2022.133764.

Gupta, V. K., Agarwal, S., Singh, P., & Pathania, D. (2013). Acrylic acid grafted cellulosic Luffa cylindrical fiber for the removal of dye and metal ions. *Carbohydr Polym*, 98, pp. 1214–1221. https://doi.org/10.1016/j.carbpol.2013.07.019.

Han, R., Zhang, L., & Song, C. (2010). Characterization of modified wheat straw, kinetic and equilibrium study about copper ion and methylene blue adsorption in batch mode. *Carbohydr Polym*, 79, pp. 1140–1149. https://doi.org/10.1016/j.carbpol.2009.10.054.

He, X., Male, K. B., & Nesterenko, P. N. (2013). Adsorption and desorption of methylene blue on porous carbon monoliths and nanocrystalline cellulose. *ACS Appl Mater Interfaces*, 5, pp. 8796–8804. https://doi.org/10.1021/am403222u.

Jabbar, A. M., & Timell, T. E. (1960). Isolation and characterization of cellulose from the inner bark of white birch (Betula Papyrifera). *Can. J. Chem.*, 38, pp. 1191–1198.

Jin, E., Guo, J., Yang, F., Zhu, Y., Song, J., Jin, Y., & Rojas, O. J. (2016). *Carbohydr. Polym.*, 143, pp. 327–335.

Lay, M., Rusli, A., Abdullah, M. K., Hamid, Z. A. A., & Shuib, R. K. (2020). Converting dead leaf biomass into activated carbon as a potential replacement for carbon black filler in rubber composites. *Composites Part B: Engineering*, 201, pp. 108366. https://doi.org/10.1016/j.compositesb.2020.108366.

Lehtonen, J., Hassinen, J., & Kumar, A. A. (2020). Phosphorylated cellulose nanofibers exhibit exceptional capacity for uranium capture. *Cellulose*, 1, pp. 1–14. https://doi.org/10.1007/s10570-020-02971-8.

Liu, Y. (2018). FT-IR spectroscopic study of cellulose. *Carbohydrate Polymers*, 195, pp. 573–584.

Luo, X., Yuan, J., & Liu, Y. (2017). Improved Solid-Phase Synthesis of Phosphorylated Cellulose Microsphere Adsorbents for Highly Effective Pb2+ Removal from Water: Batch and Fixed-Bed Column Performance and Adsorption Mechanism. *ACS Sustain Chem Eng*, 5, pp. 5108–5117. https://doi.org/10.1021/acssuschemeng.7b00472.

Ma, H., Burger, C., Hsiao, B. S., & Chu, B. (2012). Nanofibrous micro-filtration membrane based on cellulose nanowhiskers. *Biomacromol*, 13, pp. 180–186. https://doi.org/10.1021/bm201421g.

Mautner, A., Maples, H. A., & Kobkeatthawin, T. (2016). Phosphorylated nanocellulose papers for copper adsorption from aqueous solutions. *Int J Environ Sci Technol*, 13, pp. 1861–1872. https://doi.org/10.1007/s13762-016-1026.

Nair, S. S. (2019). Isolation and characterization of nanocellulose from agricultural waste. *Journal of Environmental Chemical Engineering*, 7(4), pp. 103–111.

Neto, W. P. F., Putaux, J., Mariano, M., Ogawa, Y., Otaguro, H., Pasquini, D., & Dufresne, A. (2016). *RSC Adv.*, 6, pp. 76017–76027.

Noguchi, Y., Homma, I., & Matsubara, Y. (2017). Complete nanofibrillation of cellulose prepared by phosphorylation. *Cellulose*, 24, pp. 1295–1305. https://doi.org/10.1007/s10570-017-1191-3.

Noguchi, Y., Homma, I., & Watanabe, T. (2020). Properties of phosphorylated cellulose nanofiber dispersions under various conditions. *Cellulose*, 27, pp. 2029–2040. https://doi.org/10.1007/s10570-019-02922-y.

Oshima, T., Kondo, K., & Ohto, K. (2008). Preparation of phosphorylated bacterial cellulose as an adsorbent for metal ions. *React Funct Polym*, 68, pp. 376–383. https://doi.org/10.1016/j.reactfunctpolym.2007.07.046.

Rafatullah, M., Sulaiman, O., Hashim, R., & Ahmad, A. (2010). Adsorption of methylene blue on low-cost adsorbents: A review. *J Hazard Mater*, 177, pp. 70–80.

Reid, D., Laurence, W., & Mazzeno, J. (1949). Preparation and Properties of cellulose Phosphates. *Ind Eng Chem*, 41, pp. 2828–2831.

Rosa, M. F., Medeiros, E. S., Malmonge, J. A., Gregorski, K. S., Wood, D. F., Mattoso, L. H. C., Glenn, G., Orts, W. J., & Imam, S. H. (2010). Cellulose nanowhiskers from coconut husk fibers: Effect of preparation conditions on their thermal and morphological behavior. *Carbohydrate Polymers*, 81, pp. 83–92.

Sehaqui, H., De Larraya, U. P., & Liu, P. (2014). Enhancing adsorption of heavy metal ions onto biobased nanofibers from waste pulp residues for application in wastewater treatment. *Cellulose*, 21, pp. 2831–2844. https://doi.org/10.1007/s10570-014-0310-7.

Sehaqui, H., Mautner, A., & Perez De Larraya, U. (2016a). Cationic cellulose nanofibers from waste pulp residues and their nitrate, fluoride, sulphate, and phosphate adsorption properties. *Carbohydr Polym*, 135, pp. 334–340. https://doi.org/10.1016/j.carbpol.2015.08.091.

Sehaqui, H., Michen, B., & Marty, E. (2016b). Functional cellulose nanofiber filters with enhanced flux for the removal of humic acid by adsorption. *ACS Sustain Chem Eng*, 4, pp. 4582–4590. https://doi.org/10.1021/acssuschemeng.6b00698.

Sehaqui, H., Spera, P., Huch, A., & Zimmermann, T. (2018). Nanoparticles capture on cellulose nanofiber depth filters. *Carbohydr Polym*, 201, pp. 482–489. https://doi.org/10.1016/j.carbpol.2018.07.068.

Sharma, P., Kaur, H., Sharma, M., & Sahore, V. (2011). A review on applicability of naturally available adsorbents for the removal of hazardous dyes from aqueous waste. *Environ Monit Assess*, 183, pp. 151–195.

Sreekumar, P. A. (2018). FT-IR spectroscopy of cellulose and nanocellulose. *Spectrochimica Acta Part A: Molecular and Biomolecular Spectroscopy*, 205, pp. 451–460.

Srivastava, N., Thakur, A.K., & Shahi, V. K. (2016). Phosphorylated cellulose triacetate-silica composite adsorbent for recovery of heavy metal ion. *Carbohydr Polym*, 136, pp. 1315–1322. https://doi.org/10.1016/j.carbpol.2015.10.047.

Suflet, D. M., Chitanu, G. C., & Popa, V. I. (2006). Phosphorylation of polysaccharides: New results on synthesis and characterization of phosphorylated cellulose. *React Funct Polym*, 66, pp. 1240–1249. https://doi.org/10.1016/j.reactfunctpolym.

Suflet, D. M., Popescu, I., & Pelin, I. M. (2017). Preparation and adsorption studies of phosphorylated cellulose microspheres. *Cellulose Chem Technol*, 51, pp. 23–34.

Panda, P. K. (2017). FT-IR analysis of nanocellulose isolated from agricultural waste. *Journal of Environmental Chemical Engineering*, 5(4), pp. 3471–3478.

Udongwo, A., & Folorunso, O. (2025). Resource recovery from maize biomass for the synthesis of SiO_2 nanoparticles and crystallographic analysis for possible applications. *Communication in Physical Sciences*, 12, 2, pp. 276–293.

Wang, N., Ding, E., & Cheng, R. (2007). *Polymer*, 48, pp. 3486–3493.

Wang, Y. (2019). FT-IR analysis of nanocellulose isolated from cassava peel. *Journal of Nanoparticle Research*, 21(10), pp. 1–12.

Zhuang, S., & Wang, J. (2019). Removal of U(VI) from aqueous solution using phosphate functionalized bacterial cellulose as efficient adsorbent. *Radiochim Acta*, 107, pp. 459–467. https://doi.org/10.1515/ract-2018-3077.

Compliance with Ethical Standards

Declaration

Ethical Approval

Not Applicable

Competing interests

The authors declare that they have no known competing financial interests

Funding

The author declared no source of external funding

Availability of data and materials

Data would be made available on request**.**

Authors Contribution

All the authors contributed to the work**.** The corresponding author designed the work while all the authors were involved in experimental, manuscript development and corrections of the manuscript.